

*Article*

# Damping Behavior of Layered Aluminium and Aluminide Coatings on AISI 316 Austenitic Steel

Ennio Bonetti <sup>1</sup>, Enrico Gianfranco Campari <sup>2\*</sup>, Angelo Casagrande <sup>3</sup>, Giuseppe Catania<sup>4</sup> and A. Garzoni<sup>5</sup>.

<sup>1</sup>Dipartimento di Fisica e Astronomia, viale Berti Pichat 6/2, I-40127 Bologna, Italy; ennio.bonetti@unibo.it

<sup>2</sup>Dipartimento di Fisica e Astronomia, viale Berti Pichat 6/2, I-40127 Bologna, Italy; enrico.campari@unibo.it

<sup>3</sup>Dipartimento di Ingegneria Industriale, viale Risorgimento, 4 I-40136 Bologna, Italy; angelo.casagrande@unibo.it

<sup>4</sup>Dipartimento di Ingegneria Industriale, viale Risorgimento, 4 I-40136 Bologna, Italy; giuseppe.catania@unibo.it

<sup>5</sup>Dipartimento di Ingegneria Industriale, viale Risorgimento, 4 I-40136 Bologna, Italy; andrea.garzoni2@unibo.it

\* Correspondence: andrea.garzoni@unibo.it;

**Abstract:** Several coatings configurations of combined aluminizing and diffusion layered aluminide on 316 steel were produced and characterized. These coatings, typically employed as thermal barrier coating (TBC), can also be effective as vibration reduction elements at intermediate and high temperatures. This preliminary work has been focused on the microstructural design and processing effects of the coatings. The damping of the produced specimens was measured up to 450°C and compared with that of the steel substrate. The most performing coatings contain an Al-Si layer and exhibit a steep damping increase above 200 °C, reasonably due to dislocation movements by plastic straining of soft alloy layer and to the interface sliding between layers with different elastic moduli.

**Keywords:** Aluminide; damping; coating, multilayer.

## 1. Introduction

Aluminide coatings have been extensively applied to steels and superalloys components operating in high temperature environments in order to provide thermal protection while preventing metal oxidation and hot corrosion in aggressive atmosphere [1,2]. These coatings are commonly made by refractory materials which form protective oxides. However, in many structural applications, such as mechanical systems for the aerospace, automotive and high-precision machines, materials are subjects to mechanical vibrations and noise in the low-medium temperature range, so that the performance in exercise and lifetime of operating components may differ from what expected on the base of the project specifications. Therefore, there is a growing interest in developing multifunctional coatings which can combine thermal protection and damping capabilities.

A component or a structure can attain a high damping by intrinsic or extrinsic methods. Intrinsic methods make use of the inherent ability of some materials to absorb the energy of mechanical vibrations through deformations, providing energy dissipation in the form of heat [3]. Commonly used materials for this purpose are polymers due to their viscoelastic character [4, 5]. However, viscoelasticity is not the only intrinsic damping mechanism. Defects such as dislocations, phase boundaries, grain boundaries and various interfaces also contribute. Defects may move and surfaces may slip with respect to one another during vibration, thereby dissipating energy. As a consequence, the microstructure greatly affects the damping of materials [6]. Finally, there may be a substantial dependence on temperature for all these effects. An extrinsic method can be

considered the “system damping” which is the damping due to the interactions between all the system components, that is the overall response of the structure. A good example of extrinsic damping is provided by materials in constrained layers, as in the case of multilayer coatings. Of a special interest is the use of coatings in the form of diffusion layers of metal alloys, intermetallics and ceramics applied on metallic substrates. The main contribution to damping in these systems is provided by dislocation movements by plastic straining of soft alloy layer and to the interface sliding between layers with different elastic moduli.

Unfortunately, materials which combine high damping and high stiffness are not common. A route to develop a structure or a component which exhibits high stiffness and high damping consists into creating a structure in which a damping coating and a high stiffness substrate are coupled [7]. In fact, the use of coatings, as a whole, can provide a simpler, less expensive and reliable solution with regard to an increased vibration damping of mechanical components.

The aluminide coating process used for all specimens described in this work consists of a high temperature diffusion process starting from Aluminium deposition by hot-dip process [8], followed by a thermal diffusion treatment which produces an intermetallic bond layer (Fe-Al aluminide) and a successive oxidation process to create a surface ceramic bond coat (Alumina). An AISI 316 austenitic steel substrate was used for all coatings. The different layers obtained by inter-diffusion between the substrate and the Al-rich surface, make it possible to get a continuous elastic modulus change of the final component. It is therefore possible to develop coating configurations with high damping, oxidation/corrosion resistance and a good chemical inertia. These layers, in adhesion between them and having different elastic moduli, can considerably suppress vibration and noise across a wide frequency and temperature range [9, 10]. Al-Si alloy, FeAl<sub>3</sub>, FeAl, NiAl and Alumina are the phases produced in the coatings studied in this work.

It goes without saying that the chemical-physical and mechanical properties of the adhesion interface clearly condition the damping of the system [11]. A strong adhesion of the interfaces, by inter-diffusion mechanisms, with mechanical and chemical continuity between the coating and the underneath metal, has a great influence on the damping. However, very little is known about the optimum design of layered coatings and on the damping properties of layered Fe-Aluminides at temperatures in the range 30-450 °C. Owing due to that, this paper is mainly concerned with the measure as a function of temperature of the dynamic elastic modulus and damping properties of inter-diffused layered Aluminium and aluminide coatings on a metallic substrate, compared with the uncoated component.

2. Materials and Methods

The substrate material to be subsequently aluminized is commercial AISI 316 heat-resistant steel. Its composition is listed in table 1.

Table 1. Nominal chemical composition of AISI 316 steel

Wt%	Fe	Cr	V	Ni	Mo	Mn	Si	P	Nb	Al	C	N	S	O
AISI 316	Bal	18.29	0.10	8.75	1.94	0.56	0.47	0.021	0.08	≤0.01	0.35	0.079	0.0033	0.0049

Before starting with the coating procedure, the specimens (dimensions: 50 x 5 x 0,5 mm<sup>3</sup>) were grounded up to 800-grit SiC paper and then degreased in ethanol in an ultrasonic bath for 10 min.

Layered Aluminium and aluminide coatings were produced by a hot-dipping process on sheets of AISI 316 with Al-Si hypoeutectic alloy [12] in a glove box with a furnace connected to an inert gas to minimize oxidation. All specimens were kept at 750 °C for 5 min in a bath inside an alumina crucible and were subsequently removed

and cooled in air. The bath composition of the Al-Si had a 7 % weight Si content. The thickness of the as dipped aluminized coating was about 200  $\mu\text{m}$ . The coating was formed by Al-Si alloy with an inner intermetallic  $\text{Fe}_2\text{Al}_5$  as bond coat. Both sides of metal plates have an equal layer sequence.

Six different coatings were produced:

1. as aluminized by hot-dipping (Fig. 1a), having an inner intermetallic layer and an outer Al-Si alloy layer, 200  $\mu\text{m}$  thick.
2. as aluminized by hot-dipping (Fig. 1e), having an inner intermetallic layer and an outer Al-Si alloy layer, 130  $\mu\text{m}$  thick.
3. As aluminized by hot-dipping and successively oxidized in furnace at 900 °C for 1h (Fig.1b). The resulting multilayered coating consists of an inner intermetallic Fe-Al layer, an intermediate Al-Si alloy layer and an outer Aluminium oxide layer, having about 10  $\mu\text{m}$  thickness.
4. As aluminized and then layered by a short isothermal interdiffusion process (Fig. 1f). The hot-dipped sheets where diffusion annealed at 900 °C for 3 h in a box furnace containing a metallic Titanium sheet getter in order to reduce the Oxygen content in the treating atmosphere and to promote the formation of a diffuse ion coating consisting of an inner FeAl and an outer  $\text{Fe}_2\text{Al}_5$  layer. These sheets were subsequently oxidized in  $\text{O}_2$ -rich atmosphere at 900 °C for 30 min.
5. Same thermal treatment as in 4, except that the diffusion annealing at 900 °C lasted for 4 h (Fig. 1c).
6. As aluminized and layered by extended isothermal interdiffusion process (Fig. 1d). The hot-dipped sheets where diffusion annealed at 850 °C for 50 h to complete the  $\text{Fe}_2\text{Al}_5$  transformation in FeAl and to simultaneously form a Ni-aluminide at the substrate/FeAl interface by inward Al diffusion from the coating and outward Ni diffusion from the substrate. These specimens were subsequently oxidized at 900 °C for 5 h in a box furnace. The resulting coating consists of a NiAl layer at the substrate interface, a FeAl layer on top of it and an outer  $\text{Al}_2\text{O}_3$  layer.

The six different coatings were characterized by optical microscopy (OM) with a Reichert-Jung MeF3A and by scanning electron microscopy (SEM) with a Zeiss EVO 50. Observations were carried out on: (a) a cross section of the as Aluminium-coated specimens; (b) the same specimens after the heat-diffusion treatment; (c) AISI 316 stainless steel. Etching was performed with gliceregia reagent ( $\text{HNO}_3+\text{HCl}+\text{Glycerol}$ , 1:2:1). The coatings composition, before and after the diffusion annealing, was determined by an EDS spectrometer INCA X-ACT by Oxford Instruments. The calculated semi-quantitative compositions, for each phase, were averaged out of five values. The layers stoichiometry composition before and after isothermal annealing treatments were identified, after layer by layer abrasion, by a Philips X-ray diffractometer with  $\text{Cu K}\alpha$  radiation with 0,2  $2\theta$  step size and 1 s scan step time. Dynamic elastic modulus and damping were measured in a vacuum by means of the mechanical analyzer VRA 1604 [13,14]. In the VRA apparatus, specimens are mounted in free-clamped mode and excited in flexural vibrations by means of an alternating electrical potential difference applied between the specimen and an electrode. The damping value ( $Q^{-1}$ , as the damping parameter is commonly referred to) is obtained from the envelope of the decreasing oscillation amplitude of the specimen when excitation is turned off. It is a measure of the ratio between energy dissipation and elastic energy stored in the specimen during each oscillation cycle. Therefore,  $Q^{-1} = \Delta E / (2\pi E)$  [15]. Dynamic elastic modulus is obtained from the specimen shape and resonance frequency. Specimens are kept into resonance while temperature is changing at the selected rate. The resonance frequency of all specimens is in the 200-1000 Hz range; the strain amplitude is about  $10^{-5}$ . Samples are heated from room temperature up to a maximum temperature of 780 K at 1,5 K/min rate.

### 3. Results and Discussion

#### 3.1. Microstructural characterization and composition identification

The transverse sections of hot dip aluminised AISI 316 coatings as observed in optical microscopy, are shown in Figure 1a and Figure 1e. Two layers are clearly visible: an outer layer made of Al-Si alloy and an

inner layer made of the intermetallic  $\text{Fe}_2\text{Al}_5$  [16], as also confirmed by XRD diffraction spectra (fig. 3). The layer at the steel interface is produced by inter-diffusion during the hot process, in agreement with the diffusion rate of Iron in Aluminium being faster than that of Aluminium in Iron [17]. The rugged interface between the  $\text{Fe}_2\text{Al}_5$  layer and the Al-Si layer, with tongue-like morphology, is due to an interface moving towards the liquid Aluminium, which corresponds to a solid expansion and a predominance of phase growth over dissolution. The overall thickness of the aluminised coatings is approximately 130-200  $\mu\text{m}$ . The Al-Si alloy layer produced metallographic evidence which comprises a dispersed Al-Si eutectic phase with large precipitates having the shape of needles and platelets with the same composition as the adjacent  $\text{Fe}_2\text{Al}_5(\text{Si-Cr})$  phase. These precipitates are due to dissolution and spalling of the intermetallic diffusion layer [16,17].

In order to optimise the protective coating structure, suitable heat treatments at 900°C in the furnace box were carried out after the aluminising process. The treatments, followed by natural cooling rate, yielded:

- in the case of reduced oxidation, the complete transformation, of the Al-Si alloy layer into an intermetallic  $\text{Fe}_2\text{Al}_5(\text{Si-Cr})$  layer with successive partial transformation into a softer FeAl phase, as shown in the optical micrograph of Fig 1c, in the XRD diffraction spectra of fig.4 and in the EDS analysis of Tab.2.

- In the other, formation of an alumina layer on top of the Al-Si alloy layer by oxidation in a  $\text{O}_2$ -rich atmosphere, as shown in the SEM micrograph of fig. 2a and in the EDS X-ray map of fig. 2b.

- In the case of extended isothermal interdiffusion process, a complete transformation of the intermetallic  $\text{Fe}_2\text{Al}_5(\text{Si-Cr})$  into the more ductile FeAl phase, as detected by XRD diffraction spectra, Fig. 5, by optical metallography cross section, Fig.1d, and by chemical EDS analyses, Tab. 2. During the treatment at 850 °C for 50 h, a two steps process is occurring: Aluminium diffusion across the coating and its reaction, at the substrate-coating interface, with the alloying elements of the substrate, that is Fe, Cr and Ni. The treatment also yields, at the steel interface, an inner NiAl layer, as revealed by the optical micrograph of Fig. 1d and by the EDS chemical analysis reported in Tab.2. As a result, the coating is made of an external oxide layer, a thick FeAl intermediate layer and an inner NiAl layer with a few pores near the sample surfaces. According to the binary Al-Ni phase diagram, the Al-Ni rich region at the FeAl interface should be the ordered B2 phase [18]. This is supported by EDX data, yielding a one to one stoichiometry ratio for Ni and Al. Noteworthy, Fe has been reported to substitute for both Al and Ni sites [19].

As far as the adherence of layers to substrates and between them is concerned, the coefficient of thermal expansion (CTE) and particularly its temperature dependence becomes very important. This is because the thermal expansion mismatch between a metallic substrate and its coating generates a strain on cooling that is the primary cause of spallation of protective coatings. The average coefficients of thermal expansion for the aluminides [20] are lower than those of the AISI 316 steel ( $17 \cdot 10^{-6}/\text{K}$ ), and the same is true for the coefficient of thermal expansion of  $\text{Al}_2\text{O}_3$ , ranging from  $6,7 \cdot 10^{-6}/\text{K}$  to  $8 \cdot 10^{-6}/\text{K}$  [21] in the studied temperature range. The requirements of a thermal barrier coating system with reference to its CTE substrate are given by the following inequality:  $\text{CTE substrate} > \text{CTE aluminide bond coating} > \text{CTE oxide}$  [16]. As a consequence of that, some problems might occur in coatings with long oxidation time at temperatures as high as 850 °C since, in these conditions, the NiAl/FeAl interface shows a CTE which is lower than both that of FeAl and AISI 316 [17, 22]. The  $\alpha$ -alumina grown on the coating surface has on the other end a better adhesion to the FeAl phase owing to its rugged interface, see Figure 2a. This mechanical adhesion helps increasing the spallation resistance of coatings.



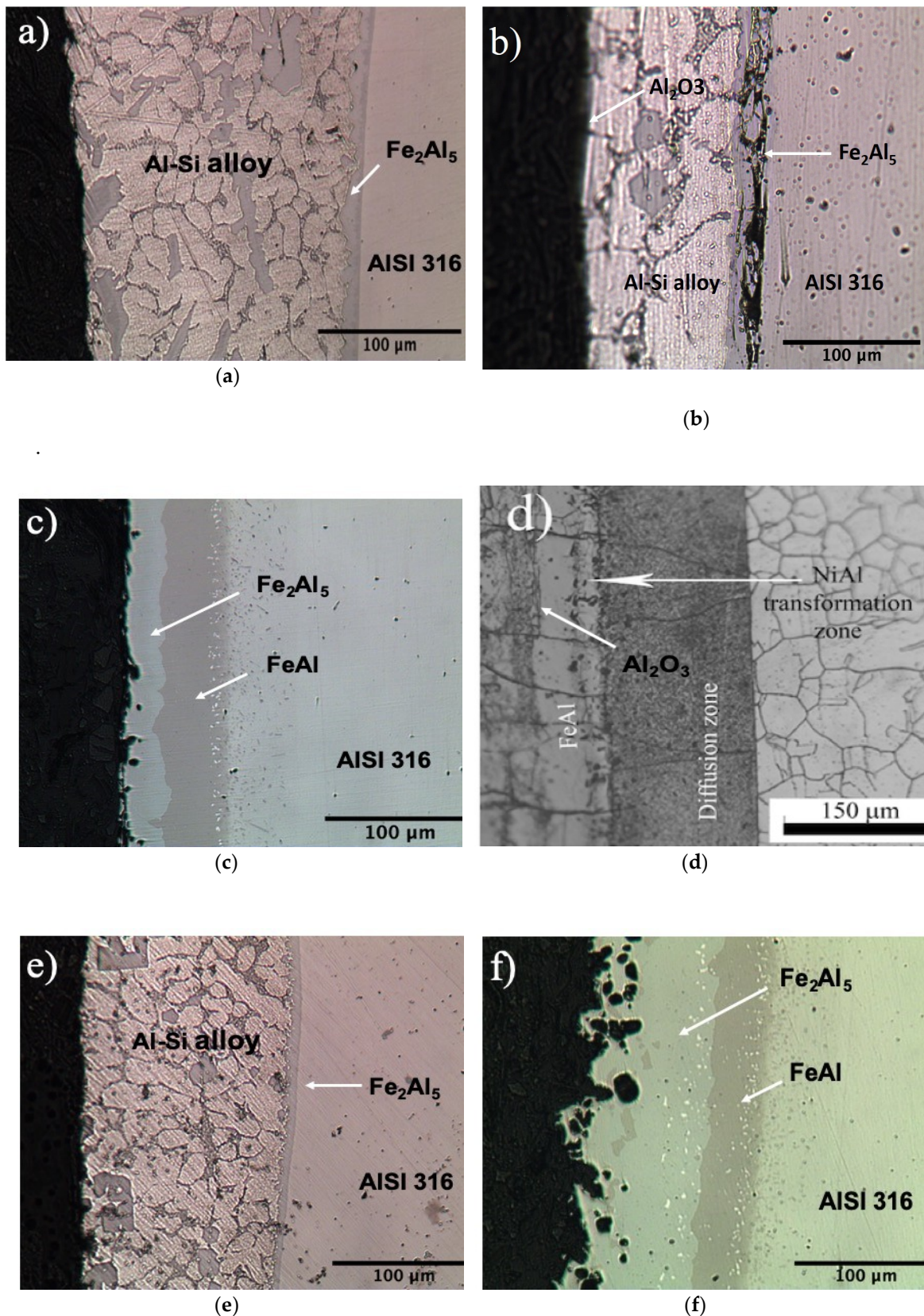


**Figure 1.** Optical microstructure of cross sections: 1a and 1e) as aluminized; 1b) as aluminized plus oxidation at 900 °C for 1 h; 1c and 1f) as aluminized and annealed at 900 °C for 3 h; 1d) as aluminized and annealed at 850 °C for 50 h.

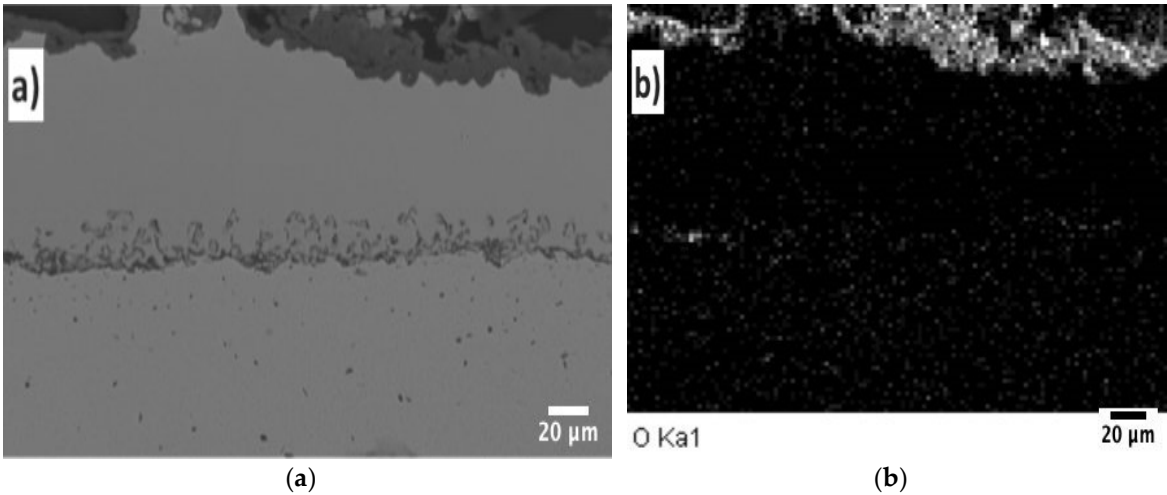


**Figure 2.** (a) SEM micrograph of cross section of specimen b of figure 1; (b) EDS X-ray map of the same specimen.

**Table 1.** Elemental semi-quantitative EDS analysis of coating layers on AISI 316.

AISI 316	O at%	Al at%	Fe at%	Cr at%	Ni at%	Si at%
Outer oxide layer	64.5	30.6	1.3	2.9		0.7
Diffusion layer (FeAl)		47.2	40.3	4.3	6.5	1.2
Intermediate Layer (Fe <sub>2</sub> Al <sub>5</sub> )		56,2	30,3	6,2		7,3
Inner layer (NiAl)		36,1	22,8	4,1	34,4	2,6
Solid solution by Al diffusion into substrate		8,4-12,1	63,6	19,1	6,6	

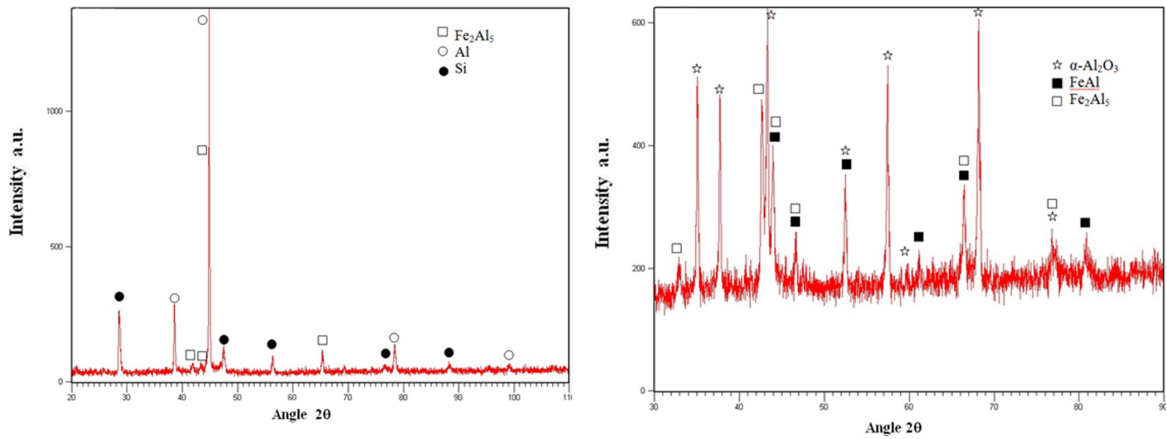


**Figure 3.** X-ray diffraction of as aluminized coating.

**Figure 4.** X-ray diffraction of diffusion aluminide coating: 900 °C for 3 and 4 h.

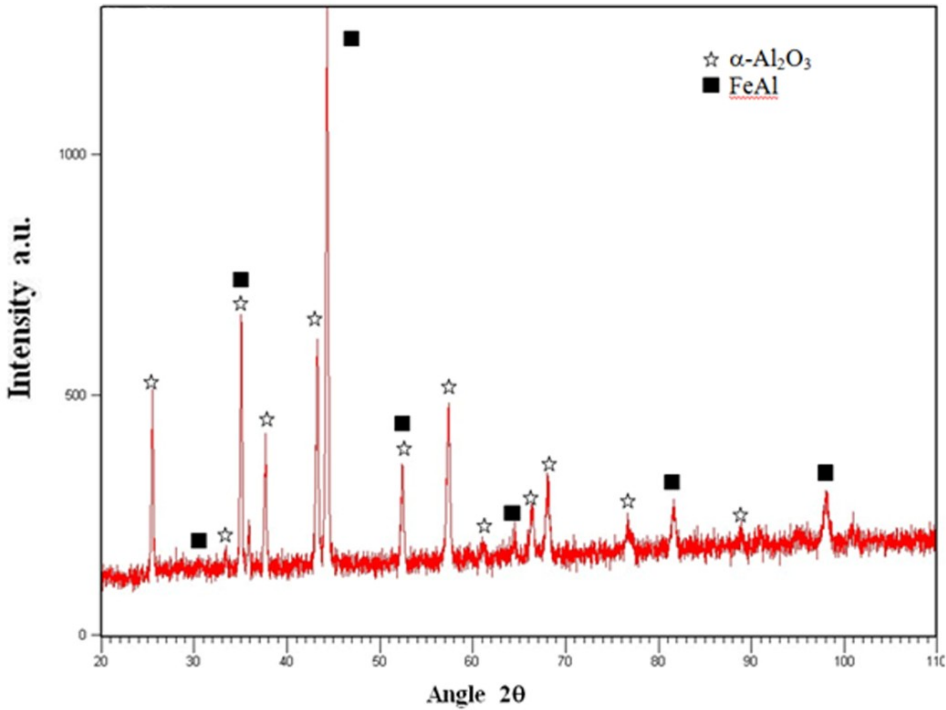


**Figure 5.** X-ray diffraction of diffusion aluminide coating: 850 °C for 50 h.

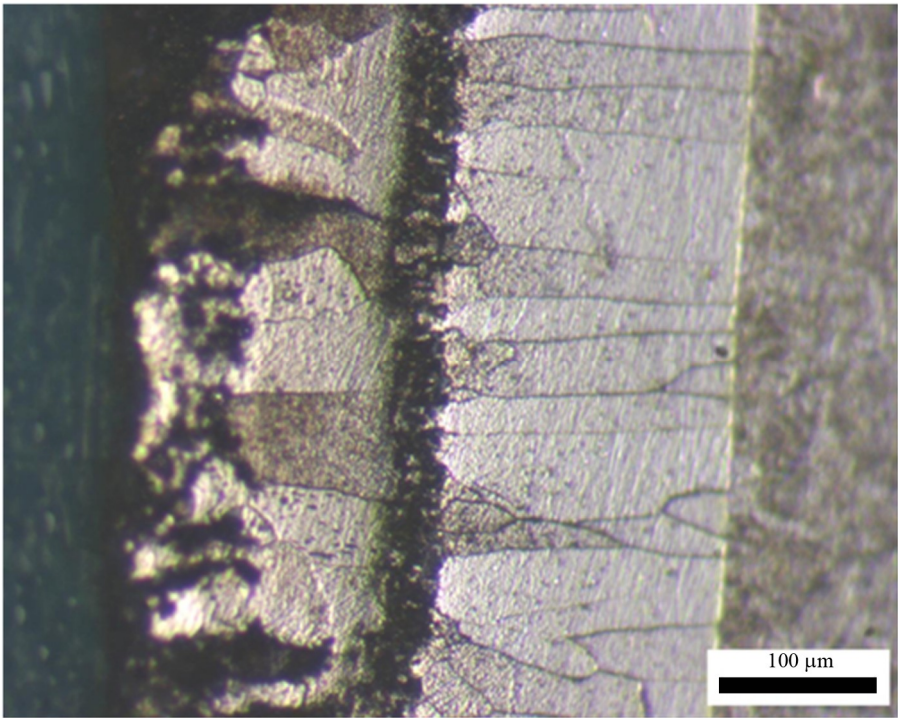




**Figure 6.** Optical microstructure of the cross section of a layered aluminide coating obtained by diffusion treatment at 850 °C for 50 h.

### 3.2. Damping behavior

Energy dissipation in industrial components is due to a combination of the following mechanisms: viscous damping, hysteretic damping, friction damping. Models can be built to simulate the overall material behavior. These cooperative models, that try to evaluate the dissipative damping behavior, become very complex when they try to simultaneously simulate multi-layered structures. This complexity stems from the variety of energy dissipation mechanisms in multi-layered structures that, in turn, depend on parameters such as frequency, amplitude and temperature. In this work, tests were carried out in the temperature range 30–450 °C in single cantilever mode with the apparatus described in the experimental procedures. The damping behavior of the multilayered structures is shown in Fig. 7. In this figure and the followings, specimens labeled from A to F have coating corresponding to those labeled from (a) to (f) in figure 1.

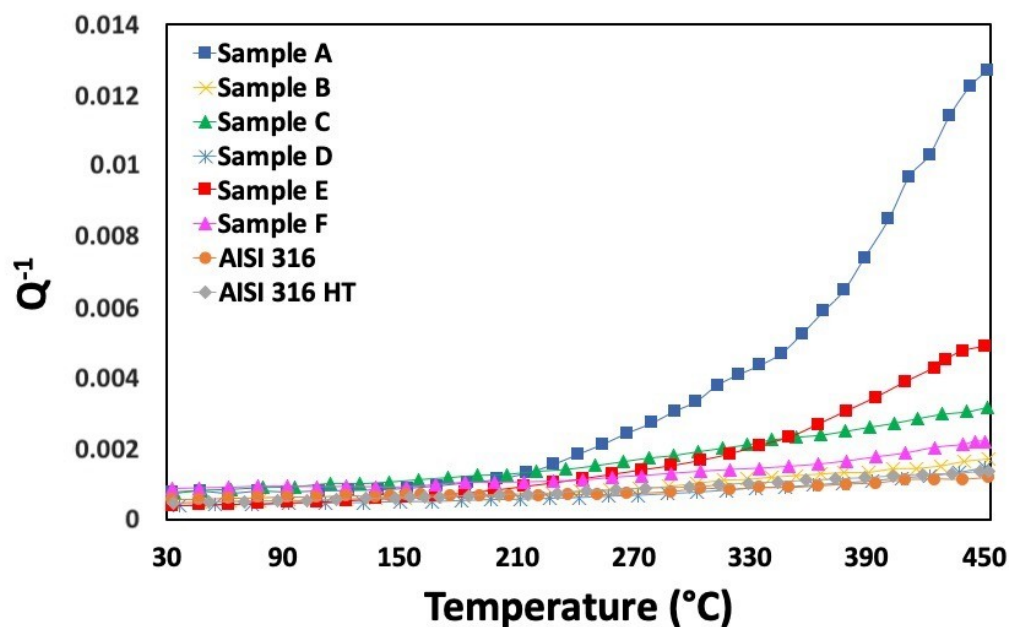


**Figure 7**  $Q^{-1}$  vs. temperature for hot dipped and thermally annealed specimens in comparison with AISI 316 steel before and after annealing to 900 C.



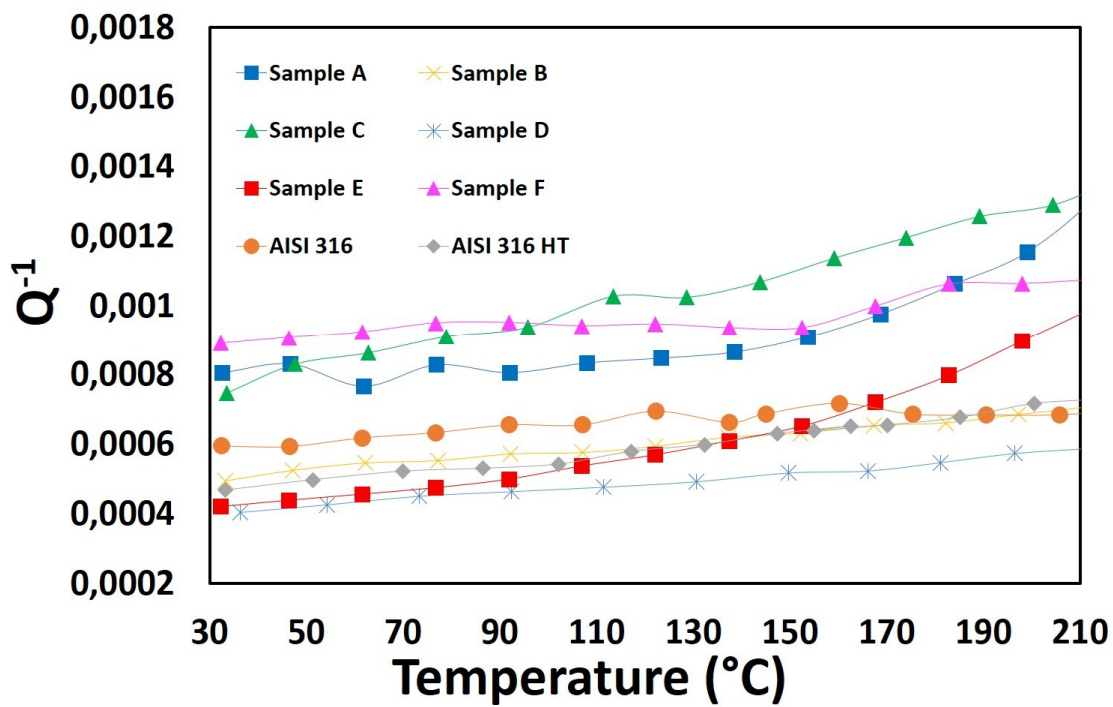


**Figure 8.**  $Q^{-1}$  vs. temperature for hot dipped and thermally annealed specimens in comparison with AISI 316 steel. Enlargement of the previous graph in the temperature range 30-210 $^{\circ}\text{C}$ .

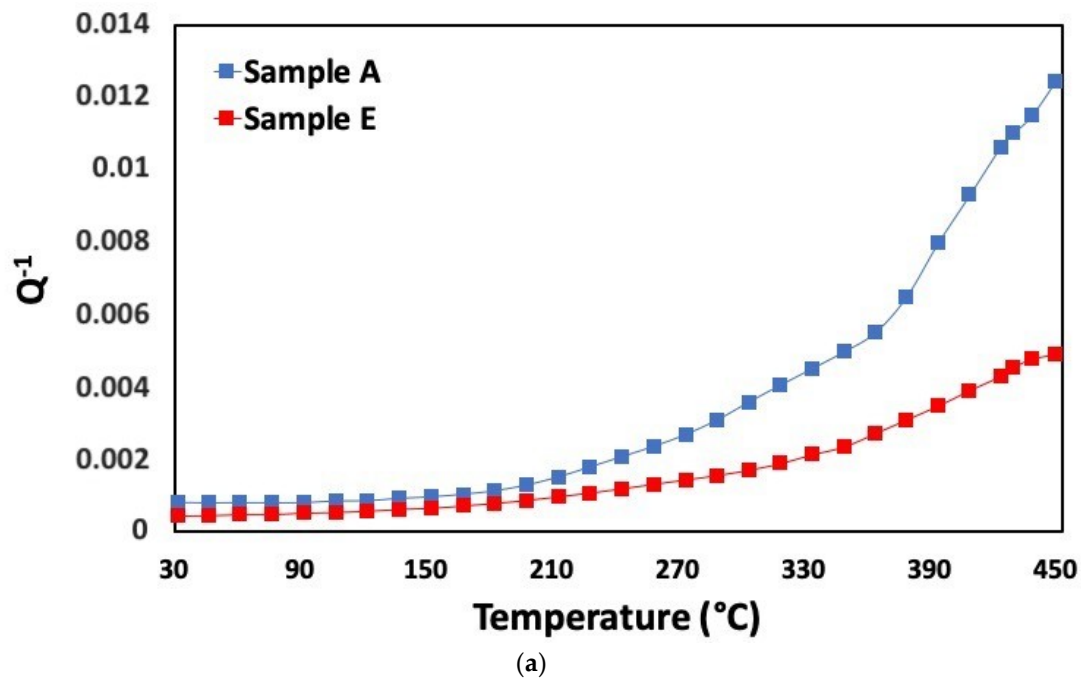


**Figure 9.**  $Q^{-1}$  vs. temperature for as aluminized specimens with different coating thickness

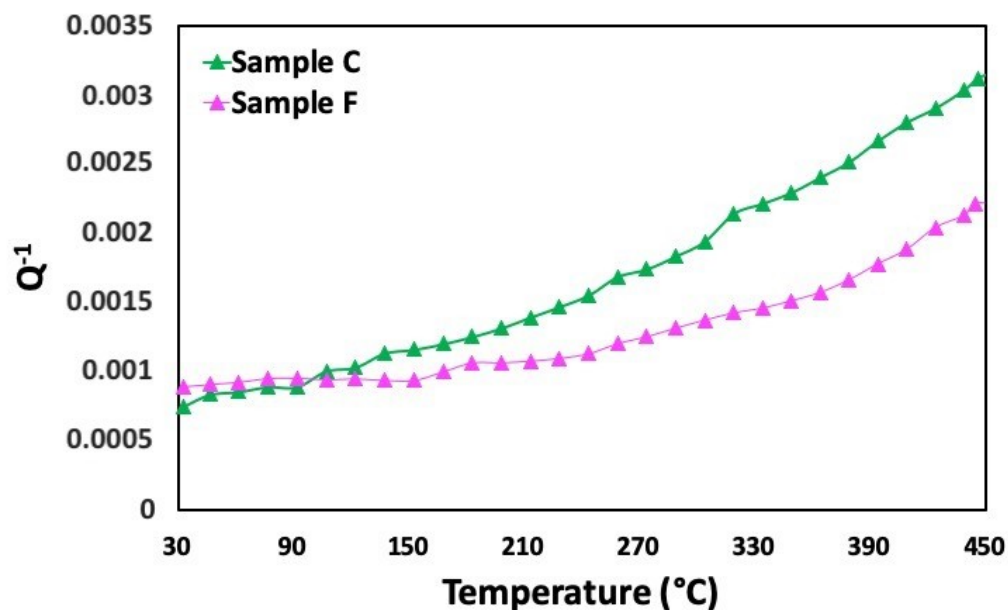


**Figure 10.**  $Q^{-1}$  vs. temperature curves for hot dipped specimens with different aluminized coating thickness and successively annealed at 900 °C for 3h and 4h, sample C and sample F respectively.

Noteworthy, all coatings exhibit, with different degrees, an increased damping with respect to that of the uncoated steel, as reported in figures 7 and 8. This increase is due to coating and becomes considerable for the case of the structure composed by a thin aluminide bond coat and an outer thick Al-Si alloy layer (specimen A and E) discrete and promising for the FeAl/Fe<sub>2</sub>Al<sub>5</sub> configuration (specimen C and F). The latter configuration exhibits two layers grown to different thicknesses by interdiffusion process. In one case the FeAl layer has a thickness of about 50  $\mu\text{m}$  while the Fe<sub>2</sub>Al<sub>5</sub> layer has a thickness of about 20  $\mu\text{m}$ , specimen C. In the other case,

specimen F, the thicknesses of the individual layers are reversed, with FeAl 30  $\mu\text{m}$  and Fe<sub>2</sub>Al 100  $\mu\text{m}$  thickness, as a result of a different time for the thermal treatment

As shown in figures 7 and 8, the damping behavior of uncoated AISI 316 and AISI 316 HT that is before and after annealing to 900 °C for 3 h, is substantially the same. In the case of the layered specimens, experimental data can be analyzed in terms of a substrate contribution plus a layer contribution. It is possible to compute the layers contribution using the equation [23]:

$$Q_f^{-1} = Q_c^{-1} + (1/(\varphi - 1))[Q_c^{-1} - Q_s^{-1}], \quad (1)$$

where the subscripts f, c and s refer to single layer, composite multilayer and AISI 316 substrate, respectively, and  $\varphi$  is:

$$\varphi = [(f_c^2 l_c^4) / (f_s^2 l_s^4)] [1 + (Q_f t_f / Q_s t_s)], \quad (2)$$

where l, t, Q, and f refer to the length, thickness, density and resonance frequency of the specimen.

This analysis allows the damping contribution of the aluminized layers to be better appreciated, as reported in figure 11 and figure 12 for specimens A and E.

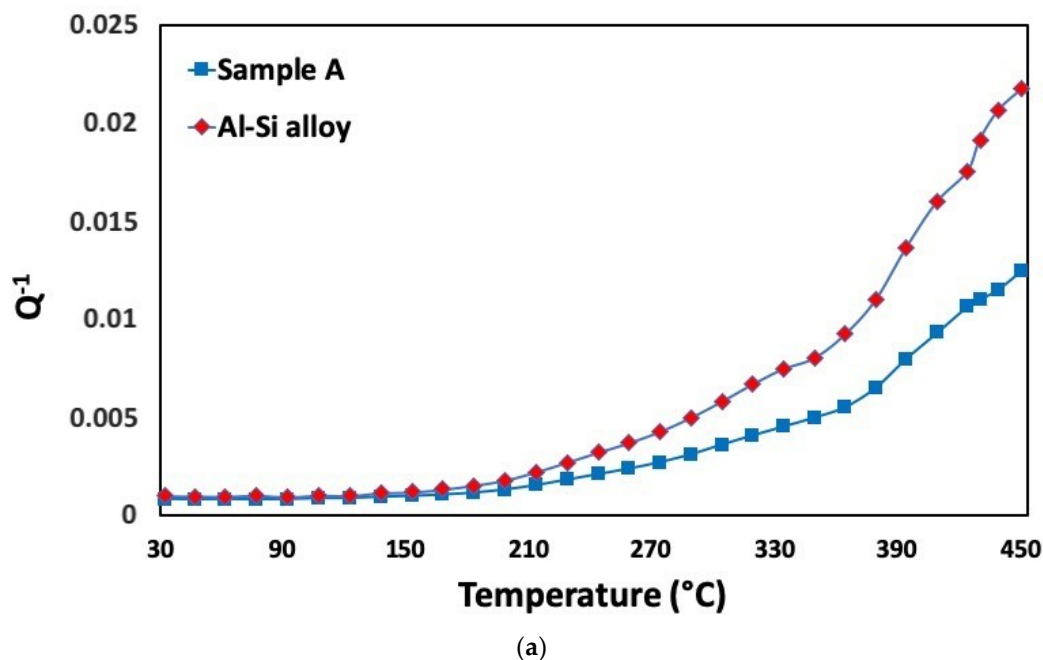


**Figure 11.**  $Q^{-1}$  vs. Temperature curves of sample A after the subtraction of the substrate contribution.

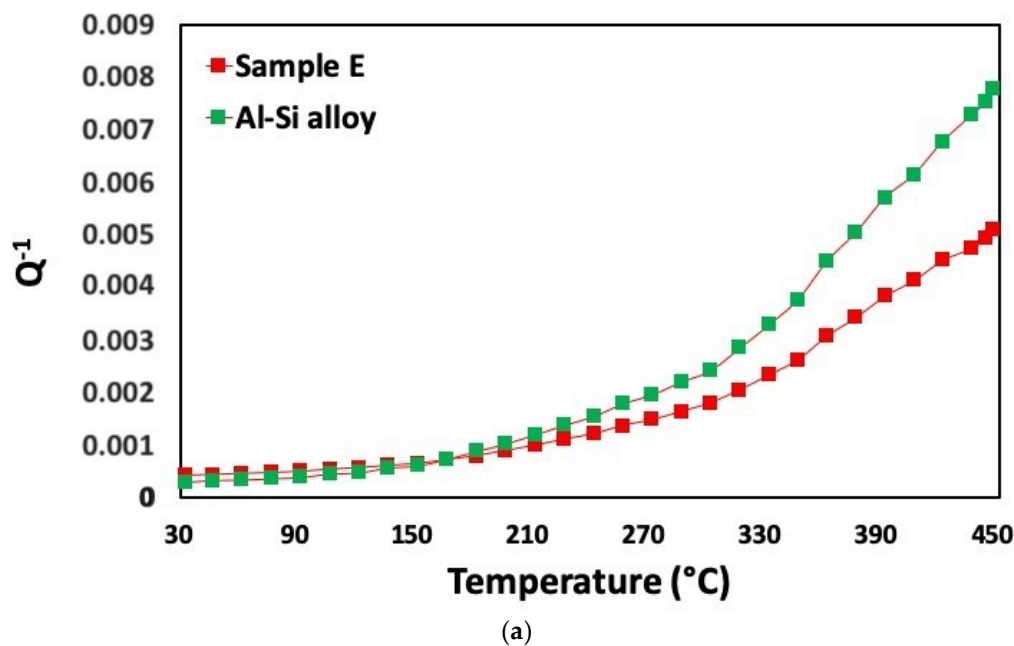


**Figure 12.**  $Q^{-1}$  vs. Temperature curves of sample E after the subtraction of the substrate contribution.

The major contribution to damping for specimens A and E is due to the Al-Si alloy layer. The elastic Young's modulus of low melting metallic alloys, such as the Al-Si alloys used to coat the AISI 316 steel, significantly decreases with a relatively small temperature increase starting from room temperature, together with the yield stress. This coating configuration possesses a high dislocation density at the interfaces, produced during the cooling process, Al-Si solidification and interdiffusion. The Internal friction fast increase above 150 °C is due to dislocation bowing and comes together with a significant reduction in elastic modulus. In this configuration, energy dissipation is due to the contribution of both viscous damping, internal damping and interface damping at the substrate/aluminide interlayer. The high local deformation in and near the interface layer can improve the damping because of the relevant energy-storing effect. In specimens C and D, thermal treatments such as keeping the specimen at 900 °C for short times, 3 and 4 h, does not lead to the complete transformation of the  $Fe_2Al_5$  intermetallic phase in the FeAl phase. The transformation being incomplete, a composition gradient is present which can hinder the bond shear strength and increase the adhesion, because the layer interfaces show a partial crystallographic coherence which opposes the crack formation.

The damping behaviour of the coating configuration of specimens C and F, as reported in figure 10, is less effective into increasing the damping in comparison with specimens A and E. The increase with temperature is not as steep as in specimen A, reasonably due to the lower dislocation density and viscoelasticity. The main contribution to damping of the coating configuration of specimens C and D is provided by the slip resistance of interfaces and by the mismatch of elastic moduli with temperature. As reported by other Authors [24], the Young's modulus of aluminides with high Al content ( $Fe_2Al_5$ ) decreases significantly when temperature is increased. Much less relevant on the contrary is the Young's modulus decrease when the aluminide (FeAl) has a lower Al content [25].

A last group of specimens is made by those annealed in oxidative atmosphere: specimens B and D, which have the following configurations: specimen B, starting from the steel interface: a fractured  $Fe_2Al_5$  layer, followed by an Al-Si alloy layer and an outer alumina layer, Fig. 1 b. Specimen D: a polycrystalline intermetallic structure made of NiAl, FeAl plus an outer alumina layer. It must be pointed out that, as expected, intermetallic layers which have a comparable Elastic Modulus do not produce a relevant damping effect [26]. The result is a moderate increased damping compared with similar configurations characterized by a low difference in CTE



between layers of Fe-Al and NiAl or alumina, figure 6. These intermetallic layers can exhibit high stress states, pores and cracks at the interfaces and do not exhibit viscoelastic behavior at room temperature. The multilayer coating of specimen D, has an internal friction comparable with that of specimen B, as reported in Fig. 7 and figure 8. This latter design should have in principle a significant damping while maintaining the same configuration of the as coated aluminized sample, with different relative thickness of the layers. Unfortunately, specimen B has a damping which is only slightly higher than that of the uncoated steel. The contribution to damping due to friction and slipping at the interface between layer seems to be negligible in this particular coating. This is reasonably due to delamination, which reduces adhesion between layers. Moreover, single polycrystalline intermetallic layers such as FeAl, Fe<sub>2</sub>Al<sub>5</sub>, NiAl show a small intrinsic damping due to the fine grain structure and the low viscoelasticity [27]. In fact, high Aluminum concentration in aluminides is detrimental to the mechanical property. Aluminum reaction with water produces Hydrogen atoms, which are in turn responsible for the low ductility of aluminides in Oxygen atmospheres [25].

The low damping can be ascribed in both kind of specimens to the weakly bonded interface between the bond coat NiAl layer and the steel substrate, Fig. 1d, and also to brittleness and cracks between the different CTE of steel and thick aluminide phase in specimen B. Finally, the grain boundary contribution to damping is, for structures with simultaneous formation of polycrystalline FeAl and NiAl, rather poor because of intrinsic brittleness when these intermetallics are not produced in an inert atmosphere. Besides that, the polycrystalline structure is heavily tensioned, resulting in poor ductility of aluminides [25].

## 5. Conclusions

A few results clearly stem from the experimental data. Above all, none of the tested multilayer coatings exhibit a significant damping increase below 200 ° C with respect to that of the substrate steel. Above that temperature, the structures which contain an Al-Si layer shows a damping exponentially increasing. Under these conditions, the predominant contribution to damping becomes viscoelastic, strongly influenced by the thickness of that layer.

The specimens having layers of Fe-Al of variable thicknesses, show very tight interfaces. This multilayer configuration shows an increased damping with respect to the reference steel, even if to a lesser extent when compared to the previous case. The main contribution to damping is now due to the sliding resistance of interfaces between layers and between the bond layer and the substrate.

No significant effects on the damping are produced by intermetallic layers such as NiAl, FeAl and Al-oxide. These ordered phases are stable up to temperatures greater than 550 ° C. Moreover, they have inconsistent interfaces due to a different crystallographic structure, highly tensioned layers, intrinsic fragility and consequently poor adhesion between layers and substrate. This kind of multilayer configuration, also due to the intrinsic layer brittleness, do not present an appreciable dislocation contribution to damping as a function of temperature.

A final consideration is that in order to maximize the adhesion between interfaces, it is necessary that intermetallic layers be as thin as possible, particularly when they act as bond layers.

**Author Contributions:** Conceptualization, E.G.C. and A.C.; methodology, E.G.C., G.C., A.C. and E.B.; validation, E.G.C., A.G.; E.B. and A.C.; data curation, A.G., A.C.; writing—original draft preparation, E.G.C., G.C. and A.C.; writing—review and editing, E.G.C. and A.C.; supervision, E.G.C. and A.C. All authors have read and agreed to the published version of the manuscript.

**Funding:** This research received no external funding.

**Acknowledgments:** CIRI-MAM of Bologna University is gratefully acknowledged for its administrative and technical support.

**Conflicts of Interest:** The authors declare no conflict of interest.

## References

- [1] G.W.Meetham, M.V.Voorde, *Materials for High Temperature Engineering Applications*; Springer, Berlin, Germany, **2000**.
- [2] David J. Young, G.C.Wood, I.G.Wright, T.Hodgkiess, D.P.Whittle, *High Temperature oxidation and corrosion of metals*, 2nd edition, School of Materials science and engineering, Univeristy of South Wales, Sydney, Elsevier Werkst. Korros. **1970** 21 p. 900;
- [3] D.D. L. Chung, *Review Materials for vibration damping*, Journal of Mat. Sci. **2001** 36, pp. 5733 – 5737. doi.org/10.1023/A:1012999616049
- [4] I.G. Ritchie and Z.L. Pan, *High-Damping Metals and Alloys*, Transactions A- Physical Metallurgy and Mater. Sci. **1991** 22A, p. 607.
- [5] E.M. Kerwin Jr. and E.E. Ungar, in *Proceedings of the ACS Division of Polymeric Materials: Science and Engineering*, Dallas, Spring 1989, ACS, Washington, DC, **1989** 60 p. 816.
- [6] R. de Batist. *High Damping Materials: Mechanisms and Applications*. Journal de Physique Colloques, **1983**, 44 (C9), pp.C9-39-C9-50. ff10.1051/jphyscol:1983904ff. ffjpa-00223326.
- [7] Griffin J.H.; *A Review of Friction Damping of turbine Blade Vibration*, Int. J. Turbo Jet Engines **1990**, 7 pp.297-308.
- [8] G.P.Cammarota, A.Casagrande, G.Sambogna, Effect of Ni, Si and Cr in the structural formation of diffusion aluminide coatings on commercial-purity titanium, *Surf. Coat. Technol.* **2006** 201 p. 230. Doi:10.1016/j.surfcoat.2005.11.125
- [9] Liming Yu, Yue Ma, Chungen Zhou, Huibin Xu; *International Journal of solids and Structures*, **2005** 42 pp.3045-3058. https://doi.org/10.1016/j.ijsolstr.2004.10.033
- [10] Piotr Matysik \*, Stanisław Józwiak and Tomasz Czujko, Characterization of Low-Symmetry Structures from Phase Equilibrium of Fe-Al System-Microstructures and Mechanical Properties, *Materials* **2015**, 8 pp.914-931; doi:10.3390/ma8030914.
- [11] J. Hu, G. Liu, S. Tang; Damping behavior in Al18B4O33w/Al composite containing an interfacial layer with low melting point metal particles, *Journal of Alloys and Compound.* **2012**, 513, pp. 61-67. doi:10.1016/j.jallcom.2011.09.073
- [12] Y. Zhang, B.A.Pint, G.W.Garner, K.M.Cooley, J.A.Haynes, Effect of cycle length on the oxidation performance of iron aluminide coatings, *Surface and Coating Technology.* **2004** 188-189 pp.35-40.
- [13] E. Bonetti, E. G. Campari, L. Pasquini, L. Savini: Automated resonant mechanical analyzer, *Rev. Sci. Instr.* **2001** 72 p. 2148, doi:10.1063/1.1357235
- [14] S. Amadori, E. G. Campari, A. L. Fiorini, R. Montanari, L. Pasquini, L. Savini, E. Bonetti, Automated resonant vibrating-reed analyzer apparatus for a non-destructive characterization of materials for industrial applications, *Materials Science and Engineering A* **2006** 442 pp.543–546, doi:10.1016/j.msea.2006.02.210.
- [15] M.S. Blanter, Igor S. Golovin, H. Neuhauser, Hans-Rainer Sinning, *Internal Friction in Metallic Glasses*, Springer Series in Materials Science, January, 2007, https://doi.org/10.1007/978-3-540-68758-0.
- [16] R.W. Richards, R.D. Jones, P.D. Clements, H. Clarke; Metallurgy of continuous hot dip aluminizing, *International Mater. Reviews*, **1994**, 39 p.191.
- [17] S.Kobayashi and T.Yakou; *Control of intermetallic compound layers at interface between steel and aluminum by diffusion-treatment*, *Material Science and Engineering, A* **2002** 338 pp.44-53.

- [18] H.C.Akuezue and D.P.Whittle; *Interdiffusion in Fe–Al system: aluminizing*, Metal Science, **1983** 17 pp.27-31. doi.org/10.1179/msc.1983.17.1.27
- [19] P.C.Tortorici and M.A.Dayananda; *Phase formation and interdiffusion in Al-clad 430 stainless steel*, Mater. Sci.Eng. A **1998** 244 pp.207-215.
- [20] M. Svec, P. Hanus, V. Vodickova; *Coefficient thermal expansion of Fe<sub>3</sub>Al and FeAl-type iron aluminides*, Manufacturing Technology **2013** 13(3) pp. 399-404.
- [21] N. Babu, R. Balasubramaniam, A. Ghosh, *High-temperature oxidation of Fe<sub>3</sub>Al-based iron aluminides in oxygen*, Corrosion Science, **2001** 43(12) pp. 2239-2254. doi.org/10.1016/S0010-938X(01)00035-X
- [22] ASM Handbook, Alloys Phase Diagrams vol.3, Materials Park Ohio 44073-0002.
- [23] Berry, B.S. Anelastic Relaxation and Diffusion in Thin-Layer Materials. In Diffusion Phenomena in Thin Films and Microelectronic Materials; Gupta, D., Ho, P.S., Eds.; Noyes Press: Park Ridge, NJ, USA, **1988**; pp. 73–145.
- [24] M. Zamanzade, A. Barnoush, C. Motz, A Review on the Properties of Iron Aluminide Intermetallics, *Crystals* **2016** 6 p.10 doi.org/10.3390/cryst6010010
- [25] M. Zamanzade, A. Barnoush, *An overview of the hydrogen embrittlement of iron aluminides*, Procedia Material Science **2014** 3 pp. 2016-2023. doi.org/10.1016/j.mspro.2014.06.325
- [26] F. Casadei, K. Bertoldi, D.R. Clarke; *Vibration Damping of Thermal Barrier Coatings Containing Ductile Metallic Layers*, Journal of Applied Mechanics **2014** 81 pp. 101001-1 – 101001-10.
- [27] Khor, K.A., Chia, C.T., Gu, Y.W. et al., High temperature damping behavior of plasma sprayed NiCoCrAlY coatings J Therm. Spray Tech. **2002** 11 pp. 359-364. Doi.org/10.1361/105996302770348745.